Solar resource-efficiency gain for energy communities based on current solar energy system deployment

David Lingfors
Uppsala University
Lägerhyddsvägen 1
SE-752 37 Uppsala
Sweden
david.lingfors@angstrom.uu.se

Johan Lindahl
Becquerel Sweden AB
Staffansvägen 14
SE-741 42 Knivsta
Sweden
johan@becquerelsweden.se

Joakim Munkhammar
Uppsala University
Lägerhyddsvägen 1
SE-752 37 Uppsala
Sweden
Joakim.munkhammar@angstrom.uu.se

Keywords

community energy systems, photovoltaics, solar energy, energy sharing, power flow analysis

Abstract

The concept of Energy Communities (EC) has been introduced in the European Union (EU) to promote energy efficiency and clean-energy transition. The EU Member States are therefore currently analysing how to promote ECs in their national context, e.g., incentive programs and juridical frameworks for internal energy sharing and providing external grid services. In Sweden, current and previous incentive programs for solar Photovoltaics (PV) have mainly been directed towards small residential, commercial or public decentralized installations, which is reflected in the high share of small systems in the Swedish PV portfolio. This study investigates the gap between the *property-optimised* and *EC-optimised* deployment of PV systems. Hence, by studying the current (property-optimised) distribution of PV, it is possible to evaluate to what extent this distribution is resource-efficient, i.e., quantify the gap to an EC-optimised distribution, where the best roofs for solar energy are utilized, in line with the goals of ECs. In a previous project, a method was developed that identifies existing Solar Energy Systems (SES), both PV and Solar Thermal, in aerial images using AI, with high precision (>95 % identified). Also, their orientation (tilt and azimuth) and impact from shading were determined based on Light Detection and Ranging data. The methodology has so far been applied to several Swedish municipalities. In this study, 20 "neighborhoods" in the Falun municipality, Sweden, defined as all customers/buildings connected to the same substation, were analysed, under the assumption to constitute hypothetical ECs. Simulated power output from actual identified PV systems, within each of these ECs, were compared to the output of PV modules hypothetically assumed to have been deployed on the "best" roof locations instead, or if "Large" roofs of high solar irradiation and low shading would have been prioritised. The voltage rises in one of the ECs were analysed through power flow analysis for these three scenarios, under the two conditions; (1) that the installed capacity of each system is fed into the grid and (2) that the actual peak power output is fed into the grid, resulting in lower voltage rises than in the first case and thereby allowing a higher PV penetration before the voltage limits are violated. The results show that shading decreased the annual yield by 12, 4 and 3 % the "Actual", "Large" and "Best" scenarios, respectively, compared to modelling without shading. The peak output is however not affected by shading. Finally, the study gives rise to some policy recommendations as a virtual EC for customers connected to the same substation is shown to be more resource-efficient in comparison to creating a parallel grid within the EC, which is currently allowed in the Swedish legislation. In addition, the substation boundary would probably simplify the dialogue between the distribution system operator and the EC, when optimising the local energy system, preferably to better match PV power generation and demand, i.e., increasing the electricity self-sufficiency, as this will benefit both parties.

Introduction

Despite market disruptions such as COVID-19, semiconductor shortages and disruptions in the value chain, the photovoltaic (PV) market is growing steadily. In 2022, a total of 236 GW of new PV capacity was installed globally (International Energy Agency, 2023), and preliminary figures show that close to 54 GW were installed in 2023 within the EU alone (SolarPower Europe, 2022). The International Energy Agency's (IEA's) latest report estimates that PV accounted for three-quarters of new renewable energy capacity installed globally by 2023 (IEA, 2023). Historically, the expected development of PV deployment has been underestimated (Jaxa-Rozen and Trutnevyte, 2021). However, a recent study suggests that solar energy will be the dominating source of energy around 2040 (Nijsse et al., 2023). Furthermore, through the EU's solar strategy, the European Commission (2022) has set the goal that over 320 GW of capacity should be in place by 2025 and almost 600 GW by 2030. As one of the cornerstones of the EU´s solar strategy, the European Solar Rooftops Initiative states the following (European Commission, 2022):

> According to some estimates, rooftop PV could provide almost 25 % of the EU's electricity consumption [Bódis et al., 2019] – this is more than the share of natural gas today. These installations – on residential, public, commercial and industrial roofs – can shield consumers from high energy prices, contributing to public acceptance of renewable energy. They can be deployed very rapidly, as they utilise existing structures and avoid conflicts with other public goods like the environment.

Among a number of action points, the European Solar Rooftops Initiative states that the installation of rooftop solar energy will be compulsory for (1) all new public and commercial buildings with useful floor area larger than 250 m^2 by 2026, (2) all existing public and commercial buildings with useful floor area larger than 250 m^2 by 2027 and (3) all new residential buildings by 2029, and that the EU and Member States will work together to set up at least one renewable-based Energy Community in every municipality with a population higher than 10,000 by 2025 (European Commission, 2022).

The concept of Energy Communities (ECs) has been implemented in EU legislation (European Parliament, 2019, 2018). Two similar concepts exist; Renewable Energy Communities (REC) from the Electricity Market Directive (EMD) (European Parliament, 2018) and Citizen Energy Communities (CEC) from the recast of the Renewable Energy Directive (REDII) (European Parliament, 2019), with similar purposes, to promote resource-efficient, democratic, just conversion and sharing of energy in local communities. Article 22, in REDII (European Parliament, 2018) states that "… Member States shall provide an enabling framework … [ensuring that] … the relevant distribution system operator cooperates with renewable energy communities to facilitate energy transfers within renewable energy communities", addressing the importance of cooperating with the Distribution System Operator (DSO). In a recent publication (Eriksson Berggren et al., 2023), the implementation of the legislation in a few northern EU countries is evaluated. So far, the legislation has been implemented to various degrees and ways in the EU Member States, and there is a lack of common understanding of what concepts and terminology should be used. Clear definitions, increased awareness and thus a regulatory framework that better enables electricity sharing are recommended (Eriksson Berggren et al., 2023).

The implementation of energy sharing, in order to increase the *Collective Self-Consumption* (CSC) of locally produced power (Giarmanà, 2023), can be administratively complex, and the most suitable sharing model may vary between countries due do existing legislations. In Switzerland (2018) and more recently in Sweden (2022), it is possible to share electricity between buildings through an internal low voltage grid (Oller Westerberg and Gustavsson, 2021). However, since this requires a parallel grid (for the existing built environment), it would probably be more cost-efficient to utilize the existing grid and share electricity virtually (Eriksson Berggren et al., 2023; Oller Westerberg, 2023). While virtual sharing of electricity can be made over large distances, the actors within a REC should be within *proximity* of the community-owned energy asset (European Parliament, 2018), where the meaning of proximity is defined nationally (European Parliament, 2018). Thus, to be in line with REDII, a natural definition of a virtual EC could be customers connected to the same medium/low-voltage substation (Oller Westerberg, 2023), which is the case in Italy (De Santi et al., 2022).

As mentioned earlier, REDII stipulates that the DSO should cooperate with the EC (European Parliament, 2018). A motivation factor for the DSO to be engaged is to increase its revenue framework by lowering the grid losses, and avoid grid reinforcements, which may be achieved if PV deployment in the EC is made wisely.

One of the advantages of sharing electricity within an EC is that the collective planning allows to maximise local power generation by PV systems by choosing the best roof(s). So far, decentralised PV systems has to a large extent been deployed as individual projects by building and property owners, which leads to an optimisation limitation as the module placements only are optimised based on the roofs within individual properties. Consequently, some of the best roofs in the EC are likely left unutilised. This study aims to investigate the difference between the *property-optimised* and *EC-optimised* deployment of PV systems. For that purpose, the power output from actual installed PV systems needs to be estimated. The DSO should have knowledge about the point of connection and maximum active power that can be fed into the grid for all grid-connected PV systems within their premises. However, for some systems the information is missing or wrong (Lindahl et al., 2023). Since smart meters, measuring the gross PV power production, are rare, and the DSO does not know the orientation (tilt and azimuth), it is difficult to estimate the actual PV power generation. Consequently, the PV self-consumption is hidden in the load data. Instead of measured PV power, the generation of individual PV systems within an area can be simulated. To be able to perform such simulations, the individual orientation of all PV systems needs to be estimated and missing/incorrectly reported installed capacity be identified. Since PV systems have distinct morphology (dark blue or black rectangles), it is suitable to use a machine learning approach to recognise patterns in aerial images in order to identify their locations. Several such approaches have been proposed recently (Frimane et al., 2023; Guo et al., 2024; Kasmi et al., 2022; Lindahl et al., 2023; Marletta et al., 2023; Mayer et al., 2020; Yu et al., 2018; Zhuang et al., 2020). Once, the exact locations of the PV systems are determined, the orientation can be derived from Light Detection and Ranging (LiDAR) data (Lingfors et al., 2018, 2017).

Method

The aim of the study is to compare the power output and grid impact of the actual deployment of PV systems to the ideal one within a hypothetical EC. As a case study, 20 hypothetical ECs were selected located in the Falun municipality, representing a mix of rural and urban settings, and in which all buildings/customers are connected to the same low voltage grid substation.

Several models had to be used to reach the goal of the study, which are briefly presented in this section. Firstly, an AI model that identifies PV systems in orthophotos is described (Lindahl et al., 2023; Mayer et al., 2020; Yu et al., 2018). Secondly, a model that estimates the tilt and azimuth of the PV systems is presented, including the assumptions made regarding shading and PV module parameters. Thirdly, three scenarios are defined, where the first represents the *Actual* deployment of PV systems, and the two latter two versions of more optimized installations for aggregated PV power generation. Finally, the procedure of the power flow analysis is outlined.

IDENTIFICATION OF PV SYSTEMS FROM AERIAL IMAGES

In order to simulate the PV power output of the actual PV systems in a realistic way, the locations and the size of the PV systems installed in an area first need to be identified and assessed. Hence, Solar Energy Systems (SES), both PV and Solar Thermal (ST), were identified in aerial images using an artificial intelligence Convolutional Neural Network (CNN) method, described in detail in Lindahl, Johansson and Lingfors (2023). In short it divides the aerial images into smaller tiles of 18.4 × 18.4 m². The model is trained on a set of such tiles, where tiles containing a PV or ST system have been manually classified. Thus, once the model has been trained, it flags tiles containing a SES if fed by a new set of tiles. The polygons representing the extent of the SES are then manually created and saved into shapefiles for further analysis. The training procedure has been repeated as more systems have been identified and in its current state, >95 % of all PV systems when a municipality is scanned are correctly identified when cross-checked against registries of the DSOs (Lindahl et al., 2023), and the now phased-out Swedish support scheme for PV (Lindahl and Oller-Westerberg, 2022). The aerial images used by the CNN model for this study, were captured in May, 2020. Since then, there has been a rapid increase in PV system uptake in Sweden, but systems installed after this date has been excluded from the study. In total 1,340 SES polygons were identified within the Falun municipality, Sweden.

ORIENTATION, SHADING AND POWER OUTPUT FROM PV SYSTEMS

The next step is to find the orientation (tilt and azimuth) of the identified PV systems. Since the buildings in the orthophotos, derived from the aerial images are not orthorectified, the roofs and the identified PV polygons will be displaced and skewed relative to their correct position and shape, respectively. This is illustrated in Figure 1, where the thick grey line represents the PV polygon in the orthophoto, which is "tilting" to the right in the image, partly outside the building footprint (thin grey line). By using LiDAR data (from the Swedish Land Survey (2023)) and the position of the air plane when the aerial image was taken, the position and shape can be adjusted, i.e., orthorectified, resulting in the polygon with the dashed white line in Figure 1.

Figure 1. Orthophoto of building with PV system (thick grey line), where the footprint is marked by a thin grey line and the PV system, after locations being corrected, with a white dashed line.

This LiDAR-based orthorectification model is currently being evaluated and is not yet described in a scientific publication, but preliminary results show that >90 % of the PV systems (in three Swedish municipalities, Falun included) get the correct azimuth from the model.

Next, using hourly Global Horisontal Irradiance (GHI) and Direct Normal Irradiance (DNI) for 2023 from the STRÅNG model (SMHI, 2015), the irradiance on the plane of array is modelled, using the Hay & Davies transposition model (Duffie and Beckman, 2013), but modified to also consider shading from surrounding objects, derived from LiDAR data (Lingfors et al., 2017). From this, the shade index, kt_s, is computed (Lingfors et al., 2017): $kt_s = I_{T,s}/I_T$, where $I_{T,s}$ and I_T is the annual solar irradiation on the tilted plane if considering and not considering shading, respectively.

The power output is modelled using the Evans model (Duffie and Beckman, 2013; Evans, 1981), in which the solar cell conversion efficiency, η_{mod}, is affected by the ambient temperature, such that:

$$\eta_{sc} = \eta_{STC}\left[1 - \mu\left(T_a - T_{sc,STC} + G_T\frac{T_{sc,NOCT} - T_{a,NOCT}}{G_{NOCT}}(1 - \eta_{STC})\right)\right], \quad (1)$$

where η_{STC} = 20 % is the solar cell conversion efficiency at Standard Test Conditions (STC), $\mu = -0.004$ °C⁻¹ is the solar cell temperature coefficient, T_a is the ambient temperature (taken from Swedish Meteorological and Hydrological Institute (2023) weather station in Falun), $T_{sc,STC}$ = 25 °C is the module temperature at STC, G_T is the irradiance on the tilted plane, $T_{sc,NOCT}$ = 45 °C, $T_{a,NOCT}$ = 20 °C and G_{NOCT} = 800 W/m² are solar cell temperature, ambient temperature and global irradiance at Normal Operating Cell Temperature (NOCT).

The power output from the module is computed, by taking the average irradiance across the module or identified PV polygon and using the Sandia inverter model (King et al., 2007), assuming 5 % losses in cables and due to soiling, snow, etc. on the direct current (DC) side, and 3.3 % losses in the inverter, but by assuming that the DC/AC ratio is 1.033, the maximum alternating current (AC) power output to the grid is the same as the installed PV capacity.

THREE SCENARIOS FOR SOLAR RESOURCE-EFFICIENCY GAIN

In this section, the specific methodology, combining the aforementioned models, is described. As motivated in the introduction section, buildings connected to the same grid substation form a natural basis for an EC. To capture the variations between such hypothetical ECs, 20 substation areas were selected in the Falun municipality on the basis of having a fairly high number of PV systems to number building ratio and such that a mix of urban and rural areas was represented. Industrial areas were neglected, since they are not targeted for ECs.

The power output from the identified PV systems was simulated as explained above forming the first *(actual)* scenario, i.e., a reference scenario, representing how the PV systems are located and performing today. The second and third scenarios were based on the potential for PV power generation on all buildings within each EC area. The orientations of each roof facet were modelled following the methodology in (Lingfors et al., 2017). In short it finds a representative roof type and tilt for each building by matching a library of template roof types to the LiDAR data within the largest rectangle contained in each building footprint.

The shading and power output were computed in the same manner as for the *actual* scenario. The model from Lingfors *et al.* (2017) deploys PV modules on *good* or *very good* parts of roofs, i.e., having an annual irradiation of >900 and >1,000 kWh/m^2, respectively. However, for the second scenario, only the *Best* module placements (i.e., with the highest annual irradiation), were considered here, forming the second scenario, corresponding to the same installed PV capacity as in the *actual* scenario. This is referred to as the *best roofs* scenario. In the third scenario, the building with the most modules classed as *very good*, is selected and filled with modules first, then the building with the second most, and so on until the same installed capacity of the other scenarios is reached. This is referred to as the *large roofs* scenario, since large roofs are prioritised. The reasons for defining this last scenario are that it is unpractical and cost-inefficient to spread out the modules on many roofs.

VOLTAGE RISE IN THE GRID

On sunny days, when the power demand is low, there will be a net flow of solar power from the PV systems towards the substation. This will give rise to increased voltage levels in the grid, especially close to the PV system, but neighbouring customers can also be affected. Before admitting the connection of a new PV system to the grid, the DSO runs a (snapshot) power flow analysis in their Network Information System (NIS). Typically, the DSO makes conservative assumptions, where the power output from the new and all other power generation under the substation is assumed to be the same as the installed capacity and that the load is zero at any given time. This will in reality never occur, but give the DSO marginal when deciding if the grid needs strengthening to comply with the grid codes before connecting the new PV system.

The most common grid code violation when introducing large shares of PV in the grid, is voltage rises (Ismael et al., 2019). To study the voltage rise in the grid, a hypothetical EC was chosen which has quite a few PV systems identified in the orthophoto and a high maximum voltage rise – at least at the point of connection of one PV system – when running a power flow simulation on the present (end of 2023) state of the grid. Once this EC was identified, the active power of the PV systems was changed to represent the simulation of the *actual* scenario for all identified PV systems. For the other PV systems that were not identified in the orthophoto, the active power was set to zero. For the *large roofs* and *best roofs* scenarios, new hypothetical PV systems had to be added to the NIS and connected to the grid. For simplicity, cables were put on the shortest path from the PV system to the prosumer's point of connection. Firstly, for all three scenarios, the power flow scenarios were run using the DSO's current policy, i.e., assuming the active power fed into the grid to be the same as the installed capacity and the load to be zero. Secondly, an additional power flow analysis was conducted in which the simulated power output from each system was chosen from the hour of the year when the total power of all the PV systems in the area was highest. Hence, this will give an idea of how conservative the current assumption of the DSO is (however, still not considering the actual load), i.e., that all PV systems will feed out power according to their nameplate inverter capacity at the same time, with no consideration taken to the different orientations of the different PV systems. For each power flow analysis, the voltage rise at each PV power system was observed. A time-series power flow analysis (considering the dynamics of load and PV power output over time) is currently not supported in the NIS, and was not conducted in this study.

Results

In this section, the results from the study are presented. First, the characteristics of the identified SES are presented. Thereafter the results from the grid analysis are described, and finally, in the third subsection, the annual yield and shading effects for all the 20 ECs are reported.

IDENTIFIED PV SYSTEMS AND SELECTED ECS

In Table 1, a summary of the characteristics of each EC is presented. As explained in the Method section, the ECs were chosen among the substation areas so that there was a reasonable number of PV systems in absolute terms, but also in relation to the number of buildings. As Table 1 shows, the number of installed PV systems by the end of 2023 (i.e., 198) was almost three times the number of identified systems in 2020 (i.e., 69), illustrating the rapid uptake of PV in Falun in recent years. The fourth EC area is marked in bold and this hypothetical EC was used for the grid impact analysis presented in the next section since there was a high voltage rise and quite a few PV systems/polygons behind this substation. The choice can be motivated by the significant uptake of PV systems in the municipality since the aerial image was produced (2020), and therefore this substation area (with a relatively high number of PV systems identified in the 2020 aerial image), would probably be representative of a typical area today.

GRID IMPACT

This section presents the resulting voltage rises in the feeder (represented by one of the ECs), when running power flow analysis for the *actual*, *large roofs* and *best roofs* scenarios, respectively. Figure 2 shows a few buildings from the EC, in which the voltage rise was analysed for the three scenarios. The actual systems, identified in the aerial images, are pointed out with white arrows in Figure 2(a). In Figure 2(b), these systems are marked with dotted lines. System 2a has a very low tilt towards the northwest and was therefore split into two, which is in line with the method for identifying the tilt and azimuth, described in the Method section; if the tilt is <5 °, and the azimuth is >60 ° off from the south, the system is split, and both parts are assigned a tilt of 10 °, but opposite azimuths. While in this case this split is incorrect, these model assumptions have proven to give correct results more often overall. This means that system 2b and half of system 2a are facing northwest, which is unfavourable in the Nordics. In the aerial image of Figure 2(a), a shadow from a tree falls on systems 2b and 2c, which have shade indices of 0.99 and 0.90, respectively. The high shade index of system 2b, means that it is almost unaffected by the tree shadow, which can be explained by the low solar irradiance when the shading occurs (early mornings). Figure 2(c) is a zoom in of system 1 and shows that system 1a is also included in the other two scenarios. In the *large roofs* scenario, a few more modules are included, which is natural, since it favours the use of large roofs. Note that the total module area in Figure 2 is not the same for the three scenarios, since the figure only illustrates a small part of the area, and thus, modules are allocated on other roofs not illustrated in the figure.

In Figure 3, the voltage rises of each scenario and PV system are presented, both if assuming that the installed nameplate capacity of all PV systems is fed into the grid at the same time (which is current practise) and peak power output in the power flow analysis which takes into account the individual orientation of all PV systems. Figure 3(a) illustrates the voltage rise for the actual PV systems, where the ellipse marks system 2 illustrated in Figure 2(a). For this system, there is a significant difference between the installed capacity (cross) and the simulated peak power output (circle) during the year, which also affects the voltage rise. For the other systems there is also a clear difference between the two settings. The difference in voltage rise decreases for the *large roofs* (Figure 3b) and *best roofs* (Figure 3c) scenarios, as the peak power output gets closer to the installed capacity. This is natural, since these scenarios are optimised for a high output and the systems are installed with azimuths towards the south and with low impact from shading. The horizontal line represents the DSOs internal voltage rise limit of 5 %. The Swedish grid code stipulates a limit of 10 %, but this is for the whole local grid, so common practise is to reserve the other 5 % upstream the substation (Energiföretagen, 2020). The markers above the horisontal line represent the same building for all scenarios, but with slightly different installed capacity. This shows that one should be careful using very large roofs or several nearby roofs as this will affect the voltage rise locally. Hence, there is a trade-off between using

Table 1. For each EC area, the number of PV systems by the end of 2023, identified PV systems in May 2020, their corresponding polygons and installed capacity, total number of buildings and if considered rural or not (i.e., urban).

EC nr	# of PV systems 2023	# of identified PV systems in 2020	# of PV polygons	Identified installed capacity (kW_p)	# of Buildings	Rural Yes/No
1	13	6	10	74.2	147	No
2	8	1	2	20.0	105	No
3	17	5	11	45.1	130	No
4	**10**	**6**	**14**	**136.7**	**183**	**Yes**
5	19	6	7	43.2	185	No
6	8	3	6	67.5	97	No
7	3	1	2	12.9	16	Yes
8	5	2	2	14.6	63	Yes
9	7	3	6	36.1	89	No
10	5	1	1	9.2	27	No
11	7	4	12	38.0	81	Yes
12	21	5	29	53.8	219	No
13	10	2	8	23.9	187	No
14	5	3	8	44.5	136	No
15	9	3	5	32.1	142	No
16	12	4	6	37.6	209	No
17	19	6	7	52.1	245	Yes
18	2	2	4	34.6	49	No
19	5	3	11	30.5	79	Yes
20	13	3	7	21.7	373	Yes
Total	**198**	**69**	**158**	**828.3**	**2,762**	**7/13**

Figure 2. (a) Aerial image of a few buildings with two rooftop PV systems. (b) Footprints of the same buildings as in (a), where (red) dotted lines represents existing "actual" PV systems identified in the aerial image. (c) Zoom in on PV system 1. In addition to the actual system, the suggested deployment of PV modules for the "large roofs" scenario (black solid lines) and the "best roofs" module scenario (grey dashed lines) are illustrated. © Swedish Land Survey.

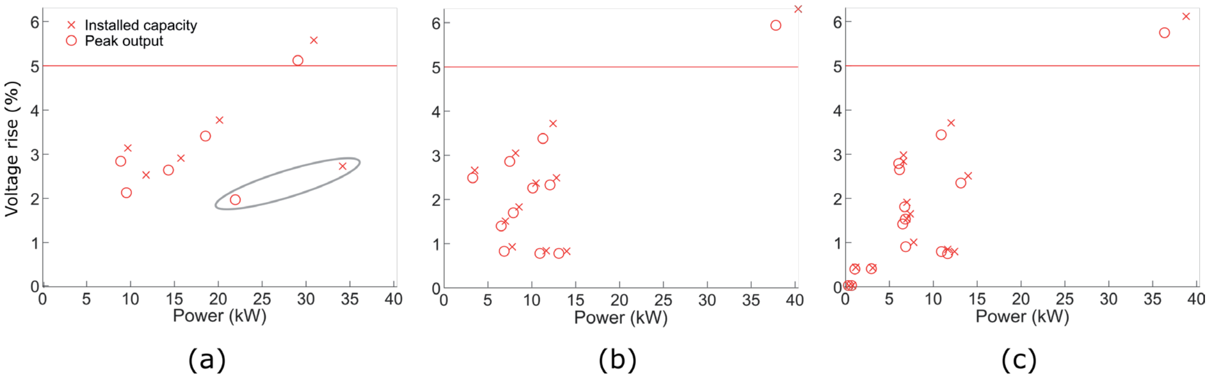

Figure 3. Voltage rise (%) as a function of considered power (kW) in the power flow analysis for (a) the "actual" scenario, (b) the "large roofs" scenario and (c) "best roofs" scenario, respectively. The horizontal line represents the voltage rise threshold according to the grid codes [3]. The considered power is either the installed nameplate capacity of the inverter (crosses) or peak power output (circles). The ellipse in (a) marks the largest deviation between these two power considerations for a single system.

large roofs for cost-efficient PV deployment and avoiding the need for grid reinforcements.

SOLAR RESOURCE-EFFICIENCY GAIN

Figure 4(a) shows the annual yield as a function of the installed capacity for the respective scenarios. Each marker represents the aggregated annual yield of all PV systems in a hypothetical EC. As explained in the Method section, the installed capacity is the same for all scenarios in an EC area, i.e., the markers are aligned vertically. The slope of the linear fit of each scenario gives an idea of the annual expected performance or *specific yield*, commonly expressed in kWh/kW$_p$. In this study it is 833, 979 and 980 kWh/kW$_p$ for the *actual*, *large roofs* and *best roofs* scenarios, respectively. The obtained specific yields in this study can be compared to an evaluation of the power generation from 828 and 1,380 Swedish PV systems during 2017 and 2018, respectively. Adjusted for the average annual global horizontal irradiation (GHI) the specific yield was 801 and 790 kWh/kW$_p$ for 2017 and 2018, respectively (Schelin, 2019). If adjusting the specific yields simulated in this study in the same manner – using STRÅNG data from 1999–2023 – the yields are 845, 993 and 994 kWh/kW$_p$, respectively. In the same study (Schelin, 2019), the specific yield for optimal orientations was simulated in PVsyst and PVGIS giving 1,006 and 939 kWh/kW$_p$, respectively, for the Dalarna county (in which Falun is located), which is in the same range as in the *large roofs* and *best roofs* scenarios and therefore validates our simulation method. However, there are several parameters that can explain the differences, such as different irradiance datasets/models and transposition models.

In Figure 4(b), the peak power output during the year is plotted as a function of the installed capacity. In addition to the linear fits, the identity line is added (thick line), indicating that the AC power output (on an hourly basis) never exceeds the installed capacity in any of the ECs (i.e., no power is curtailed). This is also true if evaluating the PV systems individually. Also, the distance between the linear fit of the actual scenario and the two others is clearly lower in Figure 4(b), which can be attributed to higher shading losses in the actual scenario, as the difference in peak power when considering shading or not is negligible.

Figure 5(a) shows the mean annual yield for all twenty ECs per scenario if shading is considered or not. The loss in annual yield due to shading is unsurprisingly highest for the *actual* scenario (12 %), followed by the *large roofs* (4 %) and *best roofs* (3 %) scenarios.

Figure 5(b) is a boxplot of the shade indices, kt_s, for all systems and scenarios, respectively. It reflects the differences shown in Figure 5(a). Hence, the spread of the shade indices is wide when considering the actual system locations, indicating that shading varies significantly between systems with a median of 0.91. Roofs with high shading, disrespectable of being modelled correctly or not, are effectively excluded for the *large roofs* and *best roofs* scenarios, with median shade indices of 0.97 and 0.99, respectively. The outliers in the *best roofs* scenario are probably not modelling errors, but the orientations of these modules are so favourable that higher shading losses can be accepted.

Discussion

This study shows that there is a potential to increase the PV power yield if choosing the best roofs for solar utilisation in an area. On the other hand, this will increase the peak power, but not to the same extent as the annual yield. In the studied grid of Falun, running a snapshot power flow analysis, assuming a power output equal to the installed capacity and zero load, only

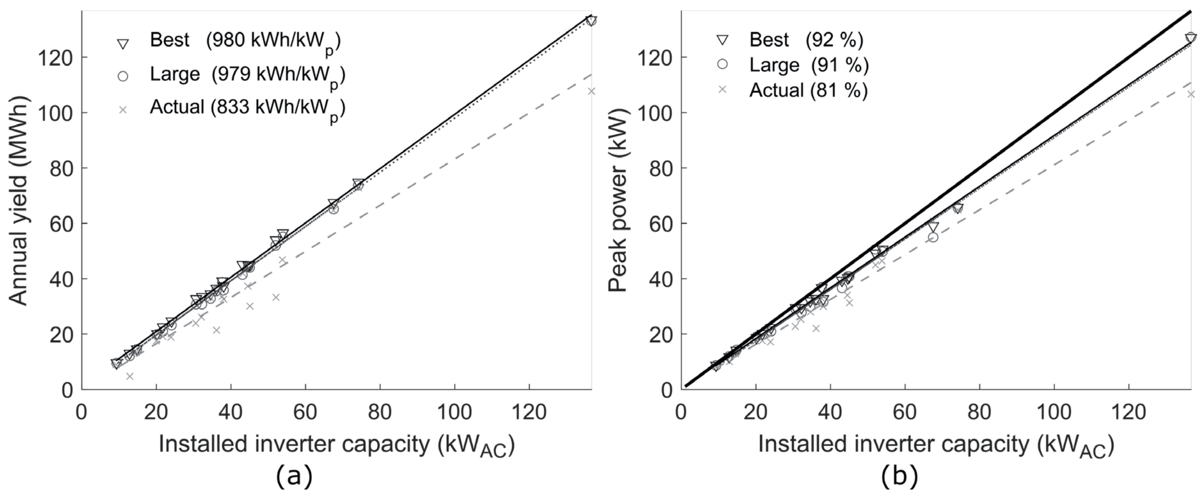

Figure 4. (a) Annual yield and (b) peak power output per EC as a function of installed inverter capacity (kW_{AC}) for each scenario. The gradient of the linear fits in (a) gives the specific yield (in parentheses in the legend) for each scenario; best roofs (thin solid), large roofs (dotted) and actual (dashed). The percentages in the legend of (b) represent the relation (linear fits) between the peak and installed power. The upper black, thick line is the identity line.

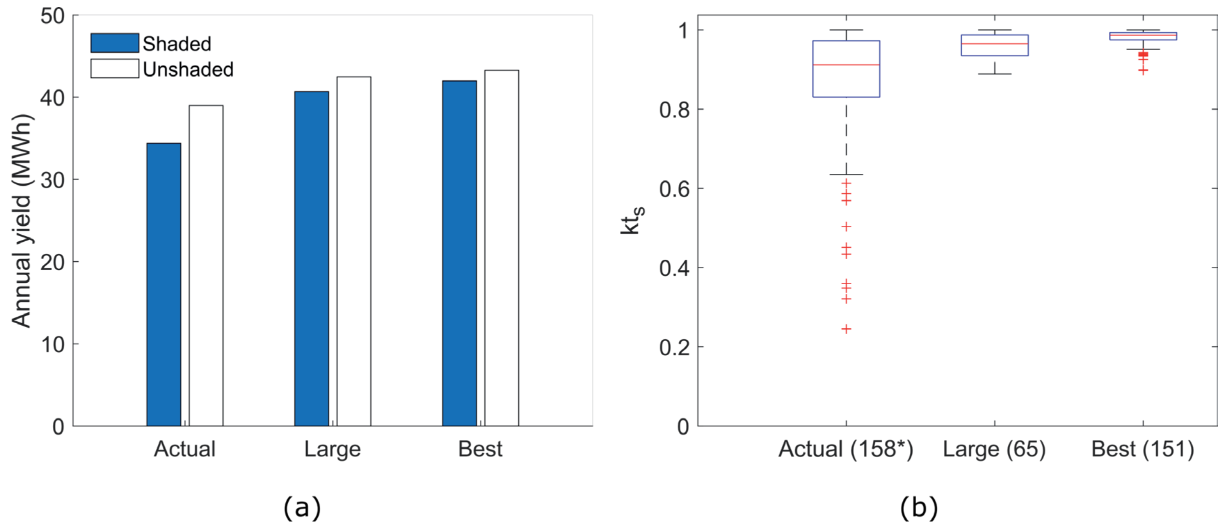

*Figure 5. (a) Annual yield if considering shading or not for the three scenarios. (b) Boxplot of the shade indices (kt_s) for each scenario. The number of buildings for each scenario is presented in parentheses. *However, for the "actual" scenario, it is the number of PV system polygons, which are distributed on 98 buildings.*

resulted in a voltage rise >5 % in very few cases and the DSO reported the need of few, if any cases, of reinforcements. However, the PV uptake is fast (59 % growth for Sweden in 2023 (Oller Westerberg and Lindahl, 2023)), and other Swedish DSOs have reported an increasing need for grid reinforcements, e.g., one of the larger DSOs, E.ON, reports that 20 % of the PV connection applications leads to further analysis (E.ON, 2024), and in the end 5 % will need grid reinforcements (E.ON, 2024; SolarPower Europe, 2022), which often takes months and sometimes up to two years to finish. Long lead times are also reported in other European countries, due to already high PV penetration or weak grid infrastructure (SolarPower Europe, 2022). Thus, estimating the peak power output, instead of assuming the installed capacity in the power flow analysis, may reduce the need for further in-depths analysis and costly reinforcements. This study is merely indicative of the potential. How the peak power should be estimated should be further analysed using time-series power flow analysis, also considering the load, preferably resulting in coincidence factor for the *netload* (load minus PV power generation), such as the *Velander constants*, historically used for the dimensioning of Swedish grids with respect to load aggregation (Velander, 1952).

Returning to the ECs, as mentioned in the introduction, a motivation factor for the DSO to engage in the planning of the energy assets, both for production and consumption and how these are distributed, is to lower the overall grid losses. Thereby, the DSO can increase their revenue framework according to rules set by The Swedish Energy Markets Inspectorate (2015), which in turn are based on the EU Energy Efficiency Directive (European Parliament, 2012). If the EC has a budget, their PV system should primarily be designed so that the self-sufficiency of the EC is maximised, since this will minimise the total load on the grid, which is proportional to the grid losses. Secondly, this means that shading losses should and probably will be kept low, since shading occurs mainly in the morning and afternoon, when all the solar power is likely self-consumed, contributing to increasing self-sufficiency.

Incentives, in both monetary terms and as information campaigns could be introduced to foster the process of finding solar resource-efficient solutions within an EC. Firstly, to raise the awareness of ECs, which in the general public is low (Eriksson Berggren et al., 2023), but also to promote dialogue between the EC, the DSO and the PV system provider.

Conclusions

In this study the peak power output and annual yield of *actual* Photovoltaic (PV) systems identified in orthophotos were simulated and compared to if re-allocated optimally, either by prioritising *large* good roofs or the very *best roofs* spots for the PV modules within hypothetical Energy Communities (ECs). Results show that the peak power output is affected by the sub-optimal orientation of the PV systems, while the annual yield is also affected by shading, i.e., 12 %, 4 %, and 3 % for the *actual, large roofs* and *best roofs* scenarios, respectively. Furthermore, if considering the peak power output instead of the installed capacity when screening for grid issues through power flow analysis, there is room for more PV to be installed before the voltage limits are violated. Defining the hypothetical EC as the customers connected to the same substation makes a clear definition of a virtual EC, which is more resource-efficient than if creating a parallel grid within the EC. Once this EC definition is in place, incentives for finding a solar resource-efficient solution both for the EC members (e.g., maximised self-sufficiency) and the Distribution System Operator (e.g., minimised grid losses), with aid from the PV system provider could be introduced. For instance in monetary terms and/or as information campaigns.

References

Bódis K, Kougias I, Jäger-Waldau A, Taylor N, Szabó S. A high-resolution geospatial assessment of the rooftop solar photovoltaic potential in the European Union. Renew Sustain Energy Rev 2019; 114: 109309. https://doi.org/10.1016/j.rser.2019.109309.

Duffie JA, Beckman WA. Solar Engineering of Thermal Processes. 4th ed. Hoboken, NJ, USA: John Wiley & Sons, Inc.; 2013. https://doi.org/10.1002/9781118671603.

E.ON. Solceller och förstärkningar av elnätet [Solar cells and grid reinforcements] 2024. https://www.eon.se/artiklar/solceller-och-foerstaerkningar-av-elnaetet (accessed 5 February 2024).

Energiföretagen. Anslutning av produktionsanläggningar till mellanspänningsnätet – AMP [Connection of production to the medium voltage grid]. vol. 5. 2020.

Eriksson Berggren S, Witt T, Van der Linden, Erika Saes L, Edander Arvejord L, Heckenberg D, Iglauer T, et al. Energy communities. 2023. https://doi.org/http://doi.org/10.6027/NER2023-03.

European Commission. EU Solar Energy Strategy. vol. 1. 2022.

European Parliament. Directive (EU) 2019/944 on Common Rules for the Internal Market for Electricity and Amending Directive 2012/27/EU. 2019.

European Parliament. Directive (EU) 2018/2001 of the European Parliament and of the Council of 11 December 2018 on the promotion of the use of energy from renewable sources (recast). 2018.

European Parliament. Directive 2012/27/EU of the European Parliament and of the Council of 25 October 2012 on energy efficiency. 2012.

Evans DL. Simplified method for predicting photovoltaic array output. Sol Energy 1981; 27: 555–60. https://doi.org/10.1016/0038-092X(81)90051-7.

Frimane Â, Johansson R, Munkhammar J, Lingfors D, Lindahl J. Identifying small decentralized solar systems in aerial images using deep learning. Sol Energy 2023; 262: 111822. https://doi.org/10.1016/j.solener.2023.111822.

Giarmanà E. Managing renewable electricity within collective self-consumption schemes: A systematic private law approach. Renew Sustain Energy Rev 2023;188. https://doi.org/10.1016/j.rser.2023.113896.

Guo Z, Lu J, Chen Q, Liu Z, Song C, Tan H, et al. TransPV: Refining photovoltaic panel detection accuracy through a vision transformer-based deep learning model. Appl Energy 2024; 355: 122282. https://doi.org/10.1016/j.apenergy.2023.122282.

IEA. Renewables 2023. 2023.

International Energy Agency. Trends In Photovoltaic Applications 2023. 2023.

Ismael SM, Abdel Aleem SHE, Abdelaziz AY, Zobaa AF. State-of-the-art of hosting capacity in modern power systems with distributed generation. Renew Energy 2019; 130: 1002–20. https://doi.org/10.1016/j.renene.2018.07.008.

Jaxa-Rozen M, Trutnevyte E. Sources of uncertainty in long-term global scenarios of solar photovoltaic technology. Nat Clim Chang 2021; 11: 266–73. https://doi.org/10.1038/s41558-021-00998-8.

Kasmi G, Dubus L, Blanc P, Saint-Drenan YM. Towards Unsupervised Assessment with Open-Source Data of the Accuracy of Deep Learning-Based Distributed PV Mapping. CEUR Workshop Proc 2022; 3343.

King DL, Gonzalez S, Galbraith GM, Boyson WE. Performance Model for Grid-Connected Photovoltaic Inverters, SAND2007-5036. vol. 38. Albuquerque: 2007.

Lindahl J, Johansson R, Lingfors D. Mapping of decentralised photovoltaic and solar thermal systems by remote sensing aerial imagery and deep machine learning for statistic generation. Energy AI 2023; 14: 19. https://doi.org/10.1016/j.egyai.2023.100300.

Lindahl J, Oller-Westerberg A. National Survey Report of PV Power Applications in Sweden 2021. 2022.

Lingfors D, Bright JM, Engerer NA, Ahlberg J, Killinger S, Widén J. Comparing the capability of low- and high-resolution LiDAR data with application to solar resource assessment, roof type classification and shading analysis. Appl Energy 2017; 205: 1216–30. https://doi.org/10.1016/j.apenergy.2017.08.045.

Lingfors D, Killinger S, Engerer NA, Widén J, Bright JM. Identification of PV system shading using a LiDAR-based solar resource assessment model: an evaluation and cross-validation. Sol Energy 2018; 159: 157–72. https://doi.org/10.1016/j.solener.2017.10.061.

Marletta D, Midolo A, Tramontana E. Detecting Photovoltaic Panels in Aerial Images by Means of Characterising Colours. Technologies 2023;11. https://doi.org/10.3390/technologies11060174.

Mayer K, Wang Z, Arlt ML, Neumann D, Rajagopal R. DeepSolar for Germany: A deep learning framework for PV system mapping from aerial imagery. SEST 2020 - 3rd Int. Conf. Smart Energy Syst. Technol., 2020. https://doi.org/10.1109/SEST48500.2020.9203258.

Nijsse FJMM, Mercure JF, Ameli N, Larosa F, Kothari S, Rickman J, et al. The momentum of the solar energy transition. Nat Commun 2023; 14: 1–10. https://doi.org/10.1038/s41467-023-41971-7.

Oller Westerberg A. Energidelning i virtuella nät [Energy sharing in virtual grids]. 2023.

Oller Westerberg A, Gustavsson U. Lokala lågspänningsnät i Sverige – En anayls av regelverksfrågan och en sammanställning av nationella och internationella frågeställningar [Local low voltage grids in Sweden – An analysis of the regulations and a compilation of national and international. 2021.

Oller Westerberg A, Lindahl J. National Survey Report of PV Power Applications in Sweden 2022. 2023.

De Santi F, Moncecchi M, Prettico G, Fulli G, Olivero S, Merlo M. To Join or Not to Join? The Energy Community Dilemma: An Italian Case Study. Energies 2022; 15. https://doi.org/10.3390/en15197072.

Schelin E. Photovoltaic System Yield Evaluation in Sweden. Mälardalens Högskola, 2019.

SMHI. STRÅNG – a solar radiation model 2015. http://www.smhi.se/en/research/research-departments/atmospheric-remote-sensing/strang-a-solar-radiation-model-1.4893 (accessed 12 October 2015).

SolarPower Europe. Europe EU Market Outlook For Solar Power 2023–2027. 2022.

Swedish Land Survey. Laser data Download, forest. 2023.

Swedish Meteorological and Hydrological Institute (SMHI). Latest observations 2023. https://www.smhi.se/en/weather/observations/observations (accessed 4 February 2024).

The Swedish Energy Markets Inspectorate. Incitament för effektivt utnyttjande av elnätet [Incentives for efficient use of the grid]. 2015.

Velander S. Operationsanalytisk metodik vid eldistribution [operation-analytic methodology for power distribution]. 82 1952: 293–9.

Yu J, Wang Z, Majumdar A, Rajagopal R. DeepSolar: A Machine Learning Framework to Efficiently Construct a Solar Deployment Database in the United States. Joule 2018; 2: 2605–17. https://doi.org/10.1016/j.joule.2018.11.021.

Zhuang L, Zhang Z, Wang L. The automatic segmentation of residential solar panels based on satellite images: A cross learning driven U-Net method. Appl Soft Comput J 2020; 92: 106283. https://doi.org/10.1016/j.asoc.2020.106283.

Acknowledgements

The authors would like to acknowledge the financing from the Swedish Energy Agency (project ID P2023-00440). The Swedish Energy Agency had no involvement or influence in any part in the study. This work forms part of the Swedish strategic research programme StandUp for Energy. We would also like to thank Oscar Willén and Joakim Neander at Falu Energi & Vatten AB (the DSO of Falun) for their help in getting access and guidance to their NIS.